JOURNAL OF MATERIALS SCIENCE 35 (2000) 2393–2403

Assessment of geometries for determining strengths of thermoplastic vibration welds

V. K. STOKES
GE Corporate Research and Development Schenectady, New York 12301
E-mail: stokes@crd. ge.com

The effects of weld geometry on the weld strength of thermoplastic resins, as determined by tests on vibration welds of bisphenol-A polycarbonate and poly(butylene terephthalate), are evaluated by tests on three weld geometries: butt welds, butt welds between specimens of different thicknesses, and T-welds. It is shown that only butt welds provide a true measure of the inherent weldability of resins. © *2000 Kluwer Academic Publishers*

1. Introduction

The growing importance of the welding of thermoplastics in load bearing applications—such as in automotive plastic bumpers and instrument panels—is focusing attention on tests for determining weld strength. The technology of choice for welding large, flat-seamed joints in thermoplastic parts is vibration welding. While the mechanics of this process and the achievable weld strengths have been characterized during the last decade, standards for defining weld strength are currently not available. As a result, tests on specimens with different geometries are being used to assess weld strength, resulting in some confusion regarding the weldability of resins. So far, most of the weld strength data have been obtained through tensile tests on butt welds. This paper evaluates the effects of weld geometry on the strengths of vibration welds through tests on the amorphous resin bisphenol-A polycarbonate (PC) and the semicrystalline resin poly(butylene terephthalate) (PBT). The three weld geometries studied are butt welds, butt welds between specimens of different thicknesses, and T-welds. It is shown that only butt welds provide a true measure of the inherent weldability of resins.

Since it depends on weld process conditions, the weld strength of a resin is not a true material property. However, the highest achievable weld strength is a characteristic of the resin that plays a role in determining the strengths of welded joints, in a manner similar to the role played by the strength of a material in determining the strength of structures. Standard tests should determine this maximum achievable weld strength, which can then be used to design welded joints.

While the local weld strength affects joint strength, the mechanical performance of a joint depends more on the joint geometry and on the type of loading. For a given resin weld strength—even if it is substantially lower than the strength of the resin—through proper design it should be possible to achieve as high a joint strength as desired. Joint design does not normally receive adequate attention during the design phase of thermoplastic parts; joining issues—considered a part of "secondary operations"—are normally an afterthought to the part design process. Designing joints after the part has already been designed results in suboptimal joint performance. When welded joints fail, the tendency is to blame the failure on poor "weld strength." Part designers need to differentiate between joint strength—which is a part or system property—and weld strength, which is a "material" property.

2. Vibration welding process

In vibration welding, frictional work done by rubbing two parts, under pressure, along their common interface is used to generate heat to melt the interfacial material [1]. Welding is achieved by allowing the molten interfacial film to solidify. In most applications the vibratory motion is along the weld seam (Fig. 1a), at right angles to the thickness direction for straight and near-straight boundaries. This normal mode of vibration welding is now well understood. However, in many applications, such as in the welding of closed seams of box-like or tubular parts, the linear vibratory motion used for generating frictional heat occurs along the part-thickness direction (Fig. 1b). In this cross-thickness welding mode, a portion of the molten layer along the entire seam is exposed to the ambient air during each vibratory cycle. The resulting reduction in the temperature can affect weld quality [2]. Under the right conditions, very high weld strengths can be achieved—in some resins the weld strength can equal that of the base resin [2]. Cross-thickness welds do not necessarily attain the highest strengths at the same process conditions as for normal-mode welds.

Past work on welding has focused on characterizing the effects of the main weld process parameters—the weld frequency, n, the amplitude of the vibratory motion, a, the weld pressure, p_0, and the weld time—on the welding process and on the achievable weld strength for several different thermoplastics. During welding, the externally imposed interfacial weld pressure causes the molten interfacial film to flow laterally outward, thereby resulting in the two parts coming closer. The

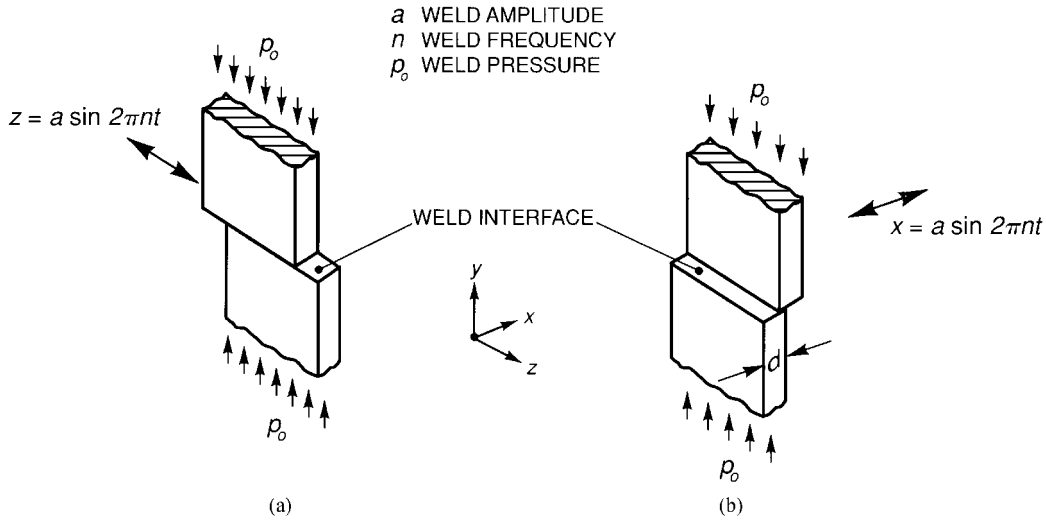

Figure 1 Diagrams illustrating normal and cross-thickness vibration welding.

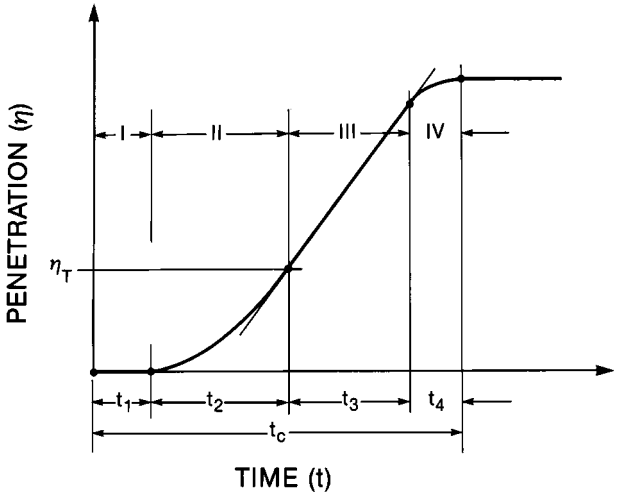

Figure 2 Schematic penetration-time curve showing the four phases of the vibration welding process.

decrease in the distance between two parts caused by this lateral outflow, called weld penetration, is useful for understanding the phenomenology of vibration welding. For neat thermoplastic resins, typical normal- and cross-thickness-mode vibration welds exhibit the four phases schematically shown [1–3] in Fig. 2. (i) In the first phase, Coulomb friction generates heat at the interface, raising its temperature to the point at which the polymer can undergo viscous flow. During this phase the penetration, $\eta = \eta(t)$, is zero. (ii) In the second phase, the interface begins to melt and the mechanism of heat generation changes from solid Coulomb friction to dissipation in the molten polymer. During this unsteady phase, in which heat is generated by viscous dissipation, lateral outflow of the molten polymer results in the penetration increasing from zero to a value η_T. (iii) In the third phase, the melting and flow attain a steady state, and the weld penetration increases linearly with time. (iv) When the machine is shut off, the weld penetration continues to increase because the weld pressure causes the molten film to flow until it solidifies. This is phase 4. The welding of dissimilar materials [4–6], chopped glass-filled materials [7, 8], and structural foams [9] also exhibit these four phases.

The most important parameter affecting the static strength of normal-mode vibration welds is the weld penetration. Static weld strengths equal to that of the resin can be achieved when the penetration exceeds a critical threshold—the penetration at the beginning of the steady-state phase—and the weld strength drops off for penetrations below this value [10, 11]. This threshold is affected by the thickness of the part being welded; the threshold increases with part thickness [12]. Additional penetration into the steady-state phase does not affect weld strength in neat resins [10, 11], in blends [11, 13], in chopped glass-filled resins [7, 8], and in structural foams [9]. However, the strengths of welds between dissimilar materials can continue to increase [4–6].

While static strength, obtained by a tensile test in which the displacement or strain or load increases at a uniform rate until failure, is an important indicator of weld quality, it is not the only measure. In some applications creep rupture may be more important, for which the time to rupture at different stress levels may be the appropriate measure of weld quality [14]. Process conditions can have a large effect on the morphology of the weld zone, which in turn can affect impact performance [15]. In some applications impact strength may therefore be a more important measure of weld quality than static weld strength. Fatigue can be important in applications involving cyclic loading; data on the fatigue strength of vibration welded butt joints for four neat resins are available [16].

3. Test geometries

The choice of a test geometry should be based on how well the stress and deformation fields at the weld interface are known during a test. From this standpoint, a tensile test on a butt weld is most attractive. The difficulty in accurately aligning thin-walled specimens during a weld has led to the consideration of other geometries such as T-joints. However, while such joints may be easier to weld and test for strength, the underlying stress fields are rather complex, so that interpretation of strength data is not straightforward.

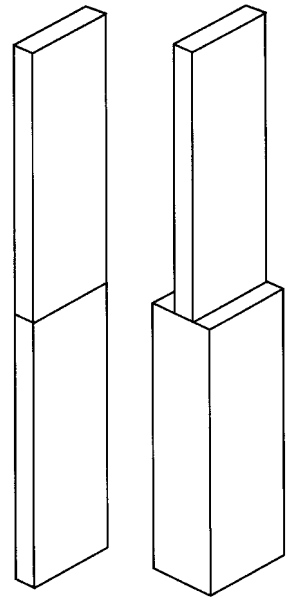

Figure 3 Butt-joint test geometries.

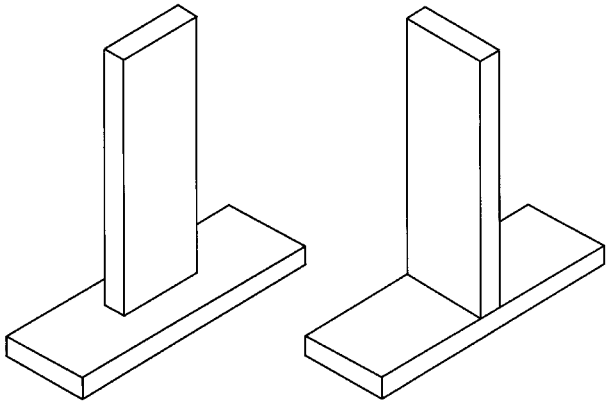

Figure 4 T-joint test geometries.

The three types of joints considered in this paper are schematically shown in Figs 3 and 4. (i) The first (Fig. 3a) is the standard butt joint geometry used in many investigations of the vibration welding process [1–13, 16]. (ii) The second (Fig. 3b) is a butt joint between two specimens of different thickness. And (iii), the third are the two T-joint geometries shown in Fig. 4.

All the tests were done using 76.2 × 25.4 mm × thickness (3 × 1 in × thickness) blocks, with machined edges, cut from sheet or from molded plaques. In the unequal thickness butt welds, the thinner specimen was centered in the center of the thicker specimen. The T-Welds were configured such that the 25.4-mm × thickness face of the first specimen was welded to the middle of the 76.2 × 25.4-mm face of the second specimen, with the 25.4-mm face of the first specimen either being aligned with 76.2-mm length of the second specimen (Fig. 4a) or normal to it (Fig. 4b).

4. Test procedure

The test data on PC were obtained from specimens cut from 3.0-mm- (0.12-in-), 5.8-mm- (0.23-in-), and 12.0-mm- (0.47-in-) thick extruded sheet material (LEXAN® 9030). The data on PBT were obtained from specimens cut from 153 × 203 mm (6 × 8 in) edge-gated injection-molded 3.2-mm- (0.125-in-) and 6.1-mm- (0.24-in-) thick plaques of VALOX® 325. The edges of each specimen were machined to obtain 76.2 × 25.4 mm × thickness (3 × 1 in × thickness) rectangular blocks for ensuring accurate alignment of the surfaces during butt welding.

Details of the weld procedure for both equal and unequal thickness butt welds are the same as those described in Ref. 10. Two specimens with machined lateral edges are vibration welded along the longitudinal (25.4-mm) direction (normal mode) or the thickness direction (cross-thickness mode) of the 25.4-mm × thickness edges, resulting in a 152.4 × 25.4-mm × thickness (6 × 1-in × thickness) bar, which is then routed down to a standard ASTM D638 tensile test specimen with the vibration-welded butt joint at its center.

These bars are then subjected to a constant displacement rate tensile test corresponding to a nominal strain rate of 10^{-2} s^{-1}. During each strength test, the average strain across the weld interface is measured with a 25.4-mm (1-in) gauge-length extensometer. Because of the local nature of failure this extensometer only establishes the lower limit of the strain at failure; the actual strain can be much higher in many cases. The weld strength reported is the load at failure divided by the cross-sectional area of the thinner specimen.

The T-joints (Fig. 4a and b) are made by clamping the flange on the stationary platen of the welding machine and vibrating the web. Here again both longitudinal and cross-thickness welds were made for both geometries. The strength of the resulting T-joint was determined by clamping the two faces of the T-flange between two plates (Fig. 5), one of which had a slot for the web of the T, and by pulling the web till failure.

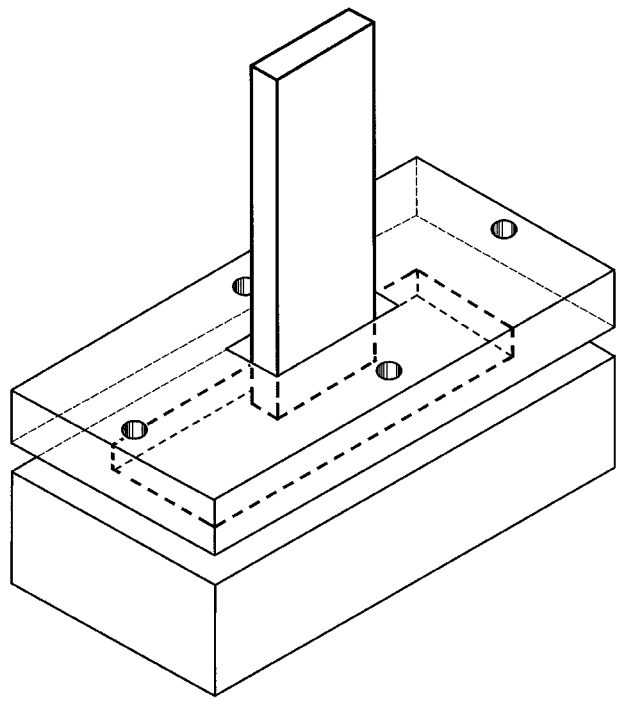

Figure 5 Fixture for determining the strengths of T-joints. The T-joint specimen is clamped between the top 51 × 102 × 12.7-mm slotted plate and the bottom 25.4-mm-thick plate by means of four 6.35-mm-diameter bolts.

The top, 51 × 102 × 12.7-mm (2 × 4 × 0.5-in) slotted clamping plate of the fixture has four 6.35-mm (0.25-in) diameter holes. T-joint specimens are clamped in place by screwing four 6.35-mm (0.25-in) bolts into tapped holes in the bottom 25.4-mm- (1-in-) thick plate. A torque wrench is used to assure uniform clamping. The bottom, 25.4-mm- (1-in-) thick clamping plate has a 25.4-mm-diameter tapped hole that is used to attach the fixture to the lower platen of the tensile testing machine. The tensile test is conducted by pulling on the exposed web of the test specimen. In this way bending is avoided during the strength test.

In these tests the clamping grip always exposes the same web length (51 mm, 2 in) above the joint. The T-joint is then pulled at a constant displacement rate corresponding to a nominal strain rate of 10^{-2} s^{-1}. During each strength test, the web displacement is monitored. The reported joint strength is the load at failure divided by the cross-sectional area of the specimen web.

All the weld tests were done at a weld frequency of 120 Hz at a weld amplitude of 1.59 mm (0.0625 in). Two weld pressures of 0.9 MPa (130 psi) and 3.45 MPa (500 psi) were used. To assess the effects of weld penetration on strength, test specimens were welded to penetration cutoffs in the range of 0.13–1.27 mm (0.005–0.050 in).

5. Process phenomenology

The weld process phenomenology for butt welds between specimens of equal thickness in these two materials is the same as in other unfilled and filled resins—the weld penetration-time curves exhibit the four phases of vibration welding, schematically shown in Fig. 1. Fig. 6 shows representative penetration-time curves for normal and cross-thickness T-welds of 5.8-mm-thick PC specimens for a weld pressure of 0.90 MPa. (Strength data for these two specimens are listed in row 8 in Table II.) The thin horizontal line corresponds to the penetration of 0.51 mm (0.02 in) at which the vibratory motion was stopped. The final penetration is higher because of continuing flow until the molten material solidifies. The corresponding penetration-time plots for

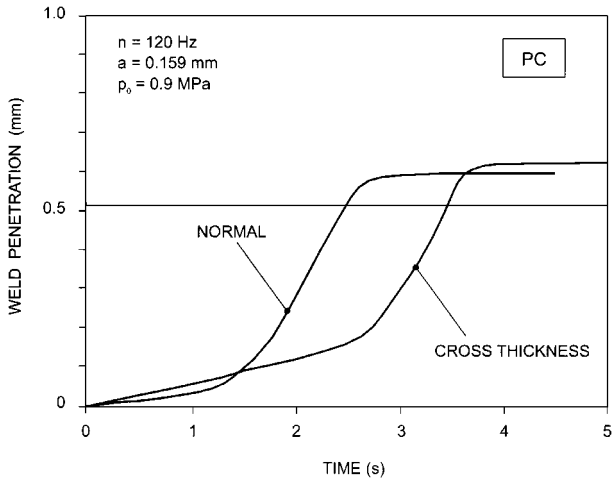

Figure 6 Representative penetration-time curves for normal and cross-thickness T-welds of 5.8-mm-thick PC.

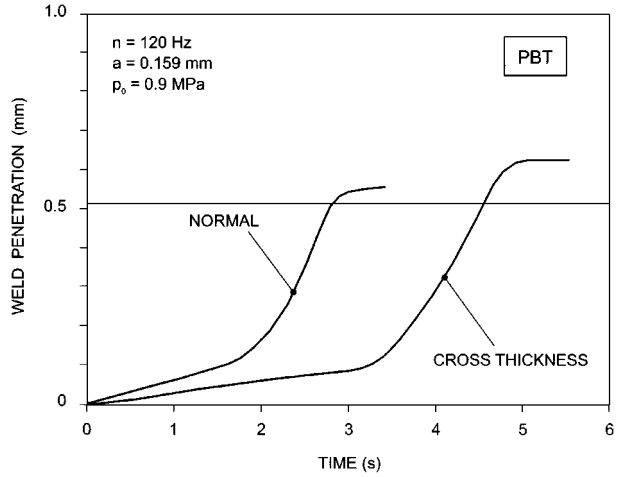

Figure 7 Representative penetration-time curves for normal and cross-thickness T-welds of 6.1-mm-thick PBT.

two 6.1-mm-thick PBT are shown in Fig. 7. (Strength data for these two specimens are listed in row 7 in Table V.) As expected, for both these materials, the cross-thickness welds require larger times to attain a prescribed penetration [2].

The penetration curves for normal mode welding clearly exhibit the four phases schematically shown in Fig. 2. The curves for cross-thickness welding also appear to attain a steady state and therefore appear to exhibit the typical four phases associated with vibration welding. The cross-thickness mode in T-joints is different from that for butt welds [2]. In the former, only the top melt surface at the edges is exposed to air during each cycle, the lower surface always being in contact with the resin. On the other hand, in cross-thickness butt welds, both surfaces get exposed to air.

For practical purposes, both normal and cross-thickness T-joints exhibit the four phases indicated in Fig. 2. The main differences are that, in cross-thickness welding, (i) it takes longer to achieve a prescribed penetration and (ii) the final penetrations are slightly higher.

6. Joint strength

The strength of a joint—the load carrying capacity of the joint—will be measured by the "average" stress at failure defined by the load at failure divided by the area of the joint. Only when the stress distribution in the joint is uniform, as in a butt joint under a uniaxial load, will this strength be a measure of the weld strength of the material. When the stress distribution is not uniform, as in a T-joint, this joint strength is a system property that depends both on the joint geometry and on the load configuration.

6.1. Strength of polycarbonate joints

For the weld process conditions used in the tests, polycarbonate butt joints between specimens of the same thickness can easily attain 100% of the strength of the base resin in both normal [10] and cross-thickness [2] modes of vibration welding.

TABLE I Strengths of polycarbonate vibration welded T-joints

T-geometry thicknesses (mm)		Weld pressure (MPa)	Weld penetration (mm)		Weld time (s)		Joint strength (MPa)		Relative joint strength[a] (%)	
Web	Flange		Normal	Cross	Normal	Cross	Normal	Cross	Normal	Cross
3.0	3.0	0.9	0.62	0.70	2.6	4.1	37.7	35.2	57	53
3.0	3.0	3.45	0.57	0.60	0.9	1.1	31.1	43.9	47	66
3.0	5.8	0.9	0.59	0.65	3.3	3.9	45.2	35.5	68	53
3.0	5.8	3.45	0.56	0.61	0.9	1.1	21.4	25.0	32	38
5.8	3.0	0.9	1.41	0.34	4.6	2.9	27.1	22.3	41	34
5.8	3.0	3.45	0.30	0.31	0.8	0.9	25.2	25.0	38	38
5.8	3.0	3.45	0.57	1.33	1.1	2.0	22.8	20.5	34	31
5.8	5.8	0.9	0.14	0.15	1.4	2.1	26.0	12.3	39	19
5.8	5.8	0.9	0.34	0.32	2.0	2.7	43.6	33.4	66	50
5.8	5.8	0.9	0.62	0.61	2.8	3.3	43.8	52.2	66	78
5.8	5.8	0.9	1.38	1.44	4.1	5.2	29.7	39.2	45	59
5.8	5.8	3.45	0.17	0.17	0.7	0.7	41.3	23.8	62	36
5.8	5.8	3.45	0.31	0.30	0.8	0.9	27.9	30.9	42	46
5.8	5.8	3.45	0.56	0.57	1.1	1.1	23.9	26.6	36	40
5.8	5.8	3.45	1.33	1.33	1.9	1.9	27.0	32.5	41	49
5.8	12.0	0.9	0.61	0.64	2.5	3.6	50.3	59.4	76	89
5.8	12.0	3.45	0.56	0.58	1.0	1.2	50.9	25.4	76	38

[a]Based on a PC strength of 66.5 MPa (9.65 ksi).

TABLE II Repeatability of polycarbonate vibration welded T-joint strengths. Repeat tests were done on T-joints with 5.8-mm-thick webs and flanges. In these 120-Hz welds the weld pressure and the weld amplitude were fixed, respectively, at 0.9 MPa and 1.59 mm

Weld penetration setting (mm)	Relative joint strength[a] (%)		Average joint strength (%)		Standard deviation (%)		Strain at maximum strength (%)		Average strain at maximum strength (%)		Standard deviation (%)	
	Normal	Cross	Normal	Cross	Normal	Cross	Normal	Cross	Normal	Cross	Normal	Cross
0.25	65.6	—					5.99	—				
0.25	63.6	—	65.9	—	1.7	—	4.37	—	5.15	—	0.66	—
0.25	66.6	—					5.13	—				
0.25	67.7	—					5.13	—				
0.51	65.8	78.4					6.71	7.45				
0.51	41.1	61.2	59.5	70.2	12.2	7.6	2.30	4.53	4.52	5.50	1.81	1.37
0.51	65.7	74.2					4.67	5.51				
0.51	65.3	66.8					4.40	4.53				

[a]Based on a PC strength of 66.5 MPa (9.65 ksi).

6.1.1. T-joints

Table I lists the strengths of several T-joints with (web, flange) thickness combinations of (3.0, 3.0), (3.0, 5.8), (5.8, 5.8), and (5.8, 12.0) mm. For each of these thickness combinations, the joints were made at two weld pressures (0.9 and 3.45 MPa), both in normal and cross-thickness welding modes. A number of different nominal penetrations (0.13, 0.51, and 1.27 mm) settings were used; they were not varied systematically except for the (5.8, 5.8) mm thickness combination. Also, the data in this table are all from one test per parameter set, and therefore do not give a feel for the scatter in the data.

Except for rows 5 and 7—for which the nominal penetrations for the normal and cross-thickness welds were (1.41, 0.34) mm and (0.51, 1.33) mm, respectively—each row in this table gives data for normal and cross-thickness welds for the same nominal penetration. For the same nominal penetration setting, the final penetration increases with the weld pressure. For the same weld process conditions, the final penetration and the weld time in the cross thickness welds are higher than in the normal welds.

The one-of-a kind data in Table I appear to indicate the following trends for relative joint strength: (i) The joint strengths are substantially lower than the achievable strength of butt welds (100%), and (ii) for a given web thickness, the joint strength appears to increase with the thickness of the flange.

To ensure that the reduced joint strengths are not artifacts of limited one-of-a-kind data, a set of five repeat tests were done for the (5.8, 5.8) mm web-flange joint combination for a weld pressure of 0.9 MPa, for two nominal weld penetration of 0.25 and 0.51 mm. The data for these repeat tests (Table II) show consistent reductions in joint strength. For the lower penetration of 0.25 mm, the joint had an average strength of 65.9%, with a small standard deviation of 1.7%. At the higher penetration, the joint strength is lower for normal welds but higher for cross-thickness welds; the standard deviations in the strengths are higher than for the lower penetration welds. These tests confirm that the reduced joint strengths are real.

This reduced strength could be ascribed to stress concentration at the joint interface induced by the reentrant corners of the T-geometry. However, remarkably, *none* of the joints failed at the weld interface. The failure surface of a T-joint with a (5.8, 5.8) mm web-flange combination is shown in Fig. 8. (The strength data for

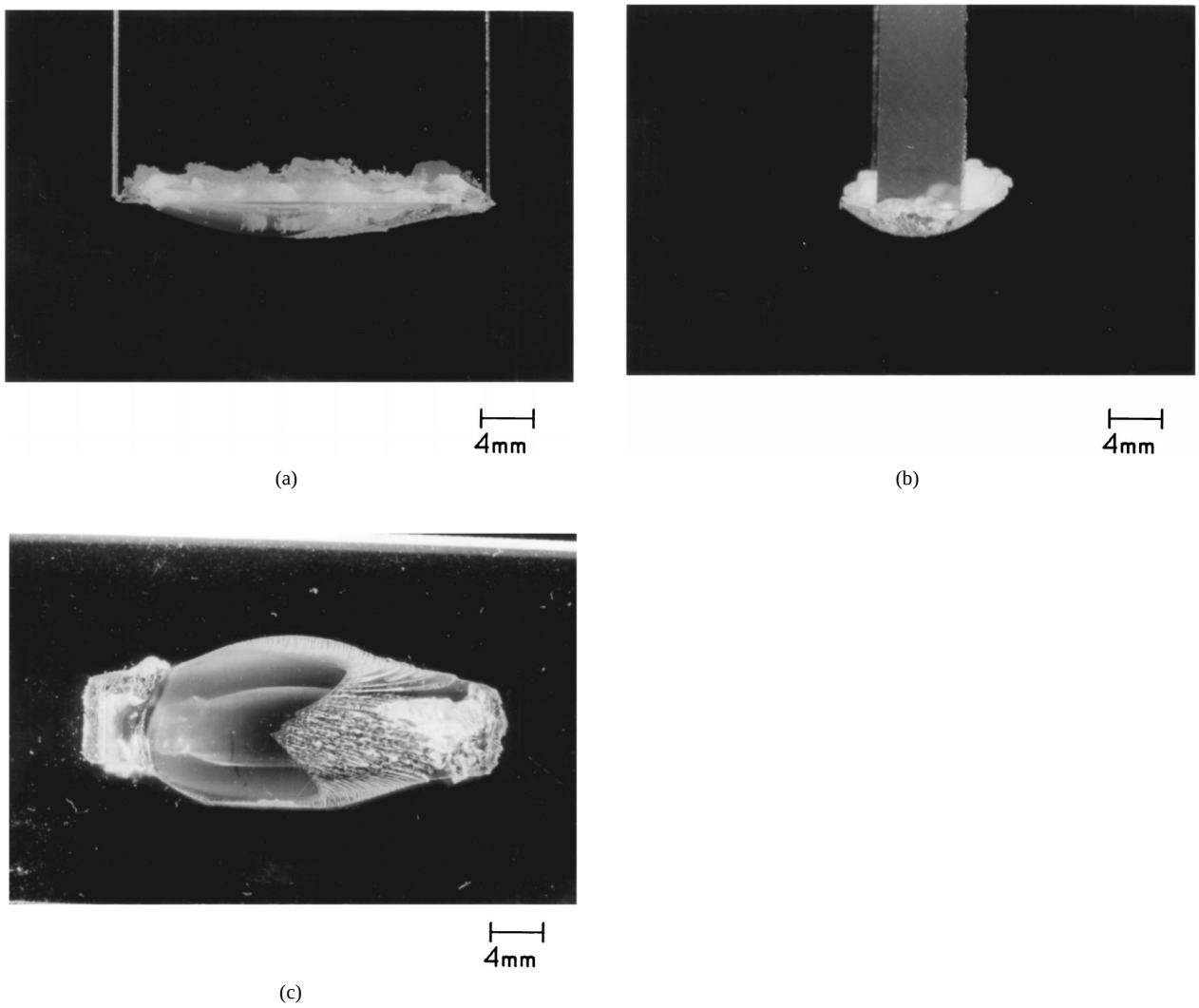

Figure 8 Failure surface of a PC (5.8, 5.8) mm web-flange combination T-joint: (a) and (b), front and side views of the web, respectively; (c), top view of the failure surface of the flange.

this cross-thickness welded T-joint are given in row 3 of Table I.) Fig. 8a and b show the front and side views of the web failure surface; Fig. 8c shows the top view of the failure surface in the flange. Clearly, the failure surface was deep into the flange.

In joints with thinner flanges, the failure surface penetrated through the flange thickness. Fig. 9 shows the side and front views (a and b) of the web failure surface, and the top view of the flange failure surface in a (5.8, 3.0) mm web-flange combination. (The strength data for this cross-thickness welded T-joint are given in row 1 of Table I.) The "punch through" in the flange is the dark trapezoidal region inside the failure surface of the flange (Fig. 9c). The reduced strength in the T-joints most likely results from the complex, three-dimensional stress state in the T-geometry.

Three-dimensional stress states are known to cause ductile resins to fail in a brittle mode [17–20]. Evidence of this mechanism being the cause of reduced strength can be seen in Fig. 10, that shows the nominal stress versus nominal strain, all the way to failure, for normal mode T-welds for a number of web and flange thickness combinations. The strength data for these specimens are listed in Table I: (3.0, 3.0) mm in row 2; (3.0, 5.8) mm in row 3; (5.8, 3.0) mm in row 5; (5.8, 5.8) mm in row 10; and (5.8, 12.7) mm in row 16. In this figure, the nominal joint stress is the tensile load divided by the cross-sectional area of the web. The nominal strain is the extension divided by 100.8 mm, the free "gauge" length of the web. Since this nominal stain is averaged over a region most of which does not fail, the actual strain at the failure site will be larger. All specimens with 3.0-mm-thick webs fail at relatively low nominal strains, while those with 5.8-mm-thick flanges fail at higher strains and stresses.

6.1.2. Unequal thickness butt joints

Strength data for butt welds of 3.0- and 5.8-mm-thick specimens to 12.7-mm-thick specimens, for weld pressures of 0.9 and 3.45 MPa and a nominal penetration of 0.51 mm, listed in Table III, exhibit relative joint strengths of about 97%, which is close to the achievable weld strength (100%) of PC. These joint strengths are much higher than those for the T-welds. The two sets of repeat tests for a weld pressure of 0.9 MPa (Table IV) confirm these high strengths. These high strengths argue against stress concentration arising from sharp

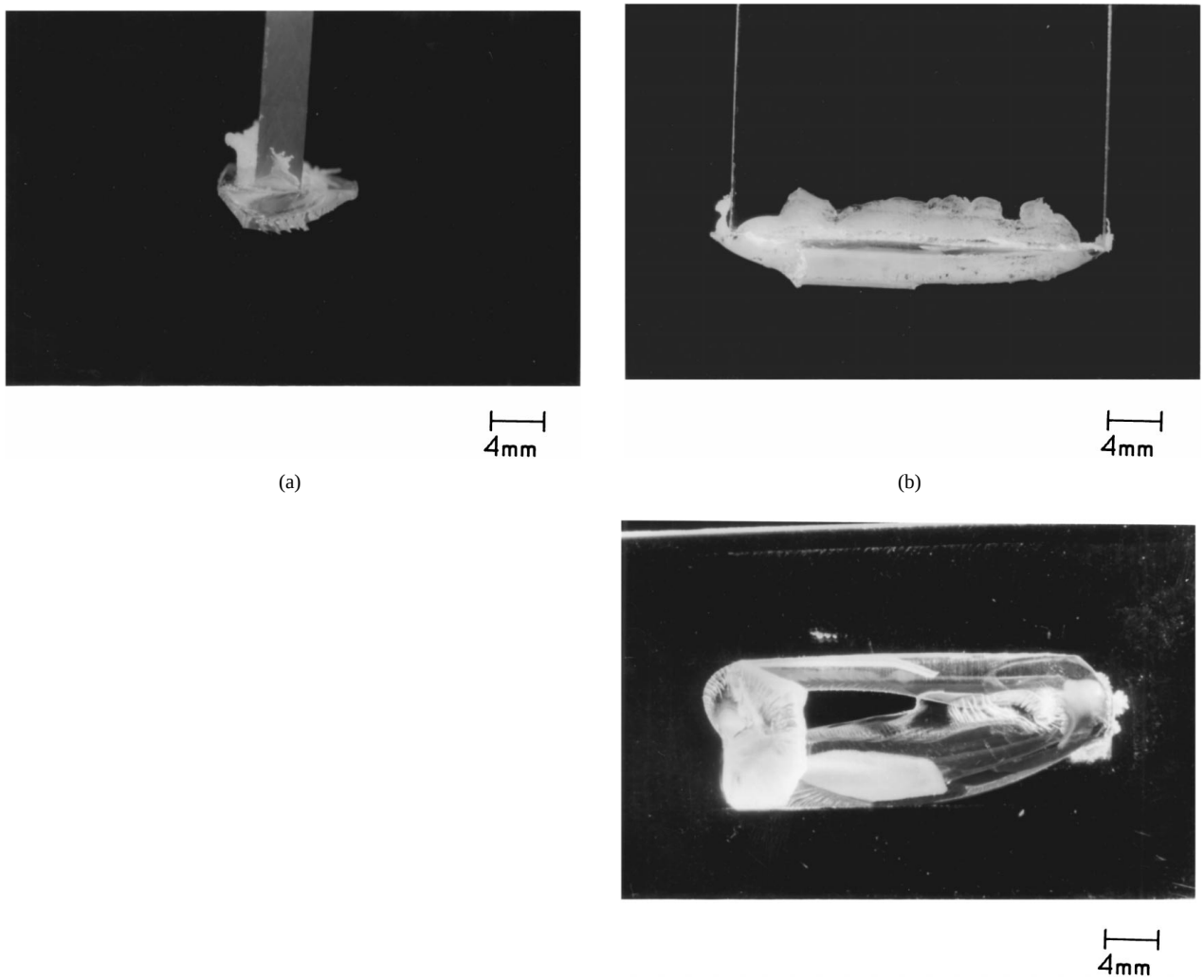

(a) (b) (c)

Figure 9 Failure surface of a PC (5.8, 3.0) mm web-flange combination T-joint. (a) and (b), side and front views of the web, respectively; (c), top view of the failure surface of the flange; the dark trapezoidal shape within the failure surface represents "punch through" of the failure surface through the bottom surface of the flange.

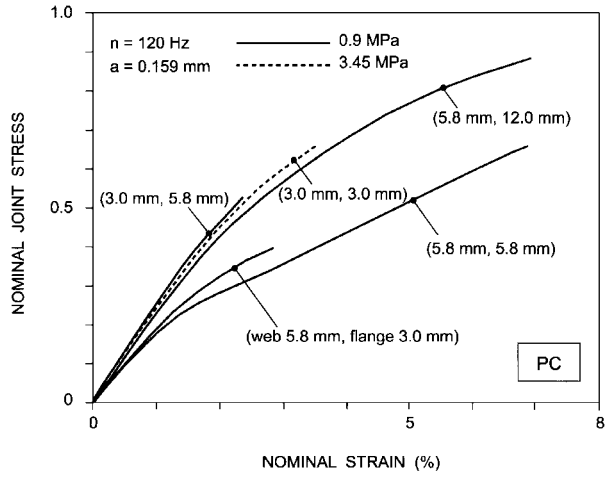

Figure 10 Nominal joint-stress versus nominal strain curves for PC for (web, flange) thickness combinations of (3.0, 3.0), (3.0, 5.8), (5.8, 3.0), (5.8, 5.8), and (5.8, 12.0) mm. Except for the curve for the (3.0, 3.0) mm combination that corresponds to a weld pressure of 3.45 MPa, all curves correspond to a weld pressure of 0.9 MPa.

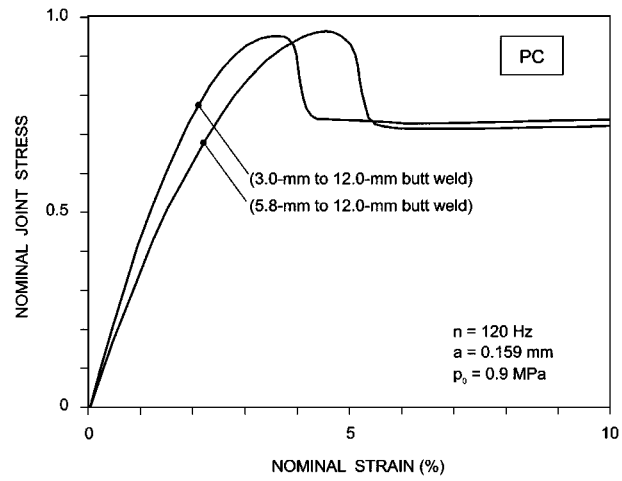

Figure 11 Nominal joint-stress versus nominal strain curves for PC for unequal thickness butt welds for (3.0, 12.0) and (5.8, 12.0) thickness combinations.

reentrant corners being the cause of the reduced strengths of T-joint welds. Fig. 11 shows the nominal stress versus nominal strain curves for (3.0-mm to 12.7-mm) and (5.8-mm to 12.0-mm) unequal welds; the corresponding strength data are listed, respectively, in rows 1 and 3 in Table III. As indicated by the sudden drop in the stress without failure, these curves confirm that these specimens fail in a ductile mode.

TABLE III Strengths of polycarbonate vibration welded butt joints between specimens of different thicknesses

Specimen thicknesses (mm)		Weld pressure (MPa)	Weld penetration (mm)		Weld time (s)		Joint strength (MPa)		Failure strain (%)		Relative joint strength[a] (%)	
Thinner	Thicker		Normal	Cross	Normal	Cross	Normal	Cross	Normal	Cross	Normal	Cross
3.0	12.0	0.9	0.57	0.71	2.2	4.3	64.5	61.3	5.10	3.52	97	92
3.0	12.0	3.45	0.57	0.57	0.7	0.9	63.0	64.1	4.23	4.73	95	96
5.8	12.0	0.9	0.59	0.60	2.0	2.9	65.1	58.0	—	3.05	98	87
5.8	12.0	3.45	0.55	0.57	0.9	1.1	64.5	65.0	4.57	5.02	97	98

[a]Based on a PC strength of 66.5 MPa (9.65 ksi).

TABLE IV Repeatability of strengths of polycarbonate vibration welded butt joints between specimens of different thicknesses. In these 120-Hz welds the weld pressure, the weld amplitude, and the weld penetration were fixed, respectively, at 0.9 MPa, 1.59 mm, and 0.51 mm

Specimen thicknesses (mm)		Relative joint strength[a] (%)		Average joint strength (%)		Standard deviation (%)		Strain at maximum strength (%)		Average strain at maximum strength (%)		Standard deviation (%)	
Thinner	Thicker	Normal	Cross	Normal	Cross	Normal	Cross	Normal	Cross	Normal	Cross	Normal	Cross
3.0	12.0	97.0	92.1					5.10	3.52				
3.0	12.0	97.8	98.5	97.3	96.2	0.4	2.8	4.53	4.81	4.6	4.4	0.4	0.6
3.0	12.0	97.5	97.0					4.64	4.65				
3.0	12.0	96.9	97.2					4.14	4.59				
5.8	12.0	97.8	87.1					—	3.05				
5.8	12.0	96.0	92.5	97.6	94.1	1.1	5.5	4.79	4.28	5.2	4.3	0.3	1.0
5.8	12.0	98.3	98.5					5.28	5.40				
5.8	12.0	98.4	98.4					5.45	4.62				

[a]Based on a PC strength of 66.5 MPa (9.65 ksi).

TABLE V Strengths of poly(butylene terephthalate) vibration welded T-joints

T-geometry thicknesses (mm)		Weld pressure (MPa)	Weld penetration (mm)		Weld time (s)		Joint strength (MPa)		Relative joint strength[a] (%)	
Web	Flange		Normal	Cross	Normal	Cross	Normal	Cross	Normal	Cross
3.2	6.1	0.9	0.58	0.68	3.4	5.1	15.6	7.1	26	12
3.2	6.1	3.45	0.55	0.61	1.2	1.7	16.4	18.0	27	30
6.1	3.2	0.9	0.59	0.57	2.8	1.7	15.7	9.0	26	15
6.1	3.2	3.45	1.30	—	2.6	—	13.3	—	22	—
6.1	6.1	0.9	0.15	0.16	1.4	3.2	9.7	8.7	16	14
6.1	6.1	0.9	0.32	0.31	2.5	3.5	14.8	13.4	25	22
6.1	6.1	0.9	0.57	0.65	2.7	4.5	16.6	17.7	28	30
6.1	6.1	0.9	1.39	1.54	4.7	6.4	18.6	14.4	31	34
6.1	6.1	3.45	0.16	0.15	0.8	0.9	16.5	12.2	28	20
6.1	6.1	3.45	0.29	0.30	1.0	1.2	25.7	19.1	43	32
6.1	6.1	3.45	0.54	0.56	1.3	1.7	15.3	11.3	26	19
6.1	6.1	3.45	1.31	1.34	2.5	2.9	17.4	14.4	29	24

[a]Based on a PBT strength of 59.8 MPa (8.67 ksi).

6.2. Strength of poly(butylene terephthalate) joints

For the weld process conditions used in the tests, PBT butt joints between specimens of the same thickness can easily attain 100% of the strength of the base resin in both normal (10) and cross-thickness (2) modes of vibration welding.

6.2.1. T-joints

Table V lists the strengths of several T-joints with (web, flange) thickness combinations of (3.2, 6.1), (6.1, 3.2), and (6.1, 6.1) mm. These data for PBT T-joints also show very low relative joint strengths—even lower than those for the PC T-joints. Here again, the failures occur in the flange thickness below the weld interface, and not in the weld, as shown by the failure surface for a (6.1, 6.1) mm web-flange combination (Fig. 12). The repeat test data for a (6.1, 6.1) mm web-flange combination for a weld pressure of 0.9 MPa and nominal penetrations of 0.25 and 0.51 mm (Table VI) confirm that this strength reduction is real and repeatable.

That failure occurs in a brittle mode can be seen from the nominal stress versus nominal strain plots for two cross-thickness T-welds, shown in Fig. 13. Failure occurs at relatively low strains. Strength data for these two welds are listed, respectively, in rows 2 and 10 in Table V.

TABLE VI Repeatability of poly(butylene terephthalate) vibration welded T-joint strengths. Repeat tests were done on T-joints with 6.1-mm-thick webs and flanges. In these 120-Hz welds the weld pressure and the weld amplitude were fixed, respectively, at 0.9 MPa and 1.59 mm

Weld penetration setting (mm)	Relative joint strength[a] (%)		Average joint strength (%)		Standard deviation (%)		Strain at maximum strength (%)		Average strain at maximum strength (%)		Standard deviation (%)	
	Normal	Cross	Normal	Cross	Normal	Cross	Normal	Cross	Normal	Cross	Normal	Cross
0.25	24.8	22.4					1.22	0.86				
0.25	30.7	27.4	28.4	28.4	5.2	5.3	1.34	1.19	1.39	1.24	0.34	0.34
0.25	23.4	28.5					1.12	1.23				
0.25	34.5	35.5					1.89	1.68				
0.51	27.8	29.6					2.20	1.47				
0.51	28.8	25.5	26.0	28.1	2.9	1.9	1.12	1.14	1.32	1.32	0.59	0.14
0.51	25.0	29.5					1.01	1.36				
0.51	22.4	27.8					0.96	1.32				

[a]Based on a PBT strength of 59.8 MPa (8.67 ksi).

TABLE VII Strengths of poly(butylene terephthalate) vibration welded butt joints between two specimens of different thicknesses

Specimen thicknesses (mm)		Weld pressure (MPa)	Weld penetration (mm)		Weld time (s)		Joint strength (MPa)		Failure strain (%)		Relative joint strength[a] (%)	
Thinner	Thicker		Normal	Cross	Normal	Cross	Normal	Cross	Normal	Cross	Normal	Cross
3.2	6.1	0.9	0.57	0.69	2.2	4.7	62.9	53.2	3.38	1.65	105	89
3.2	6.1	3.45	0.55	0.61	0.9	1.9	53.9	34.1	2.04	1.11	90	57

[a]Based on a PBT strength of 59.8 MPa (8.67 ksi).

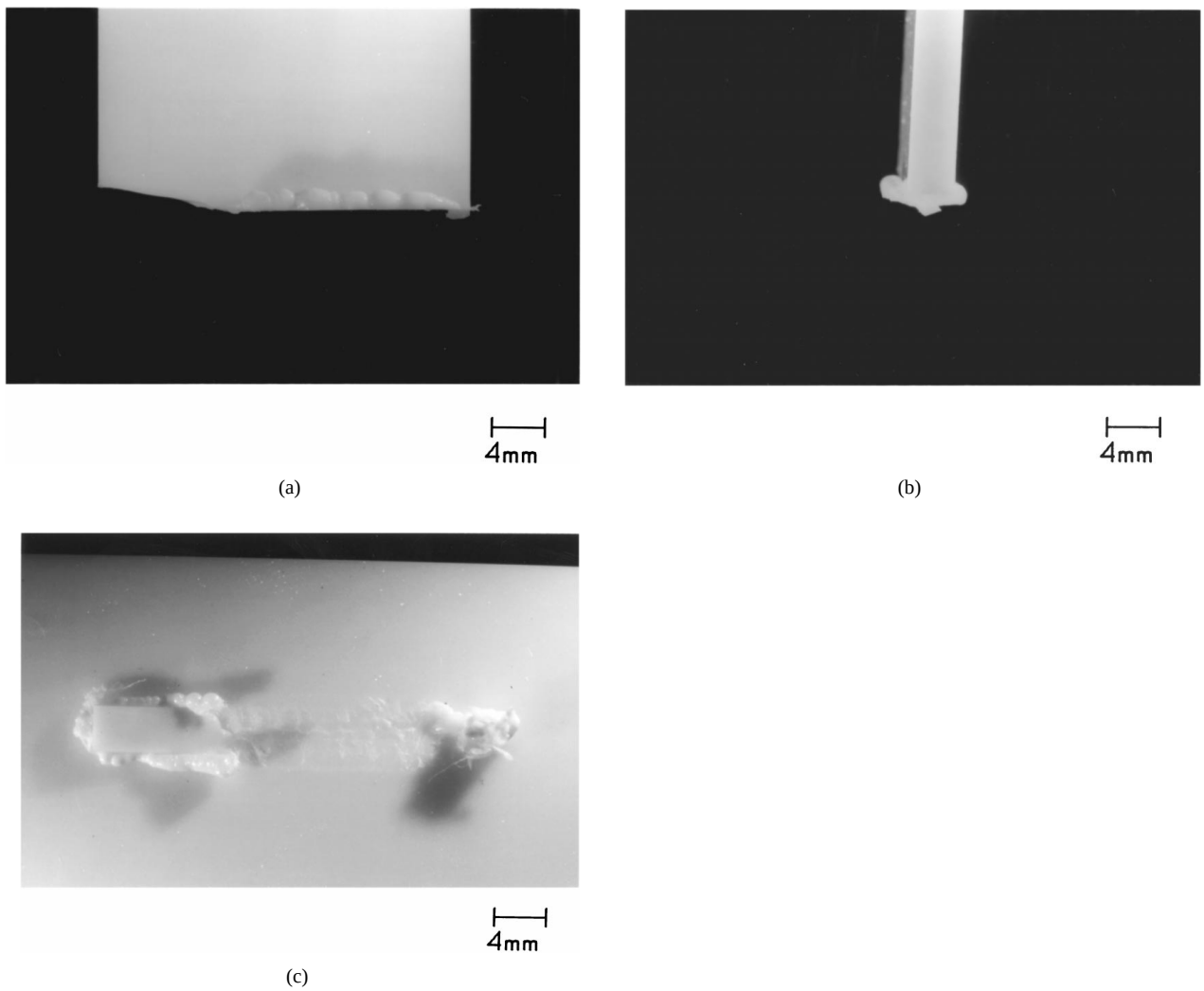

(a) (b) (c)

Figure 12 Failure surface of a PBT (6.1, 6.1) mm web-flange combination T-joint.

TABLE VIII Repeatability of strengths of poly(butylene terephthalate) vibration welded butt joints between specimens of different thicknesses. In these 120-Hz welds the weld pressure, the weld amplitude, and the weld penetration were fixed, respectively, at 0.9 MPa, 1.59 mm, and 0.51mm

Specimen thicknesses (mm)		Relative joint strength[a] (%)		Average joint strength (%)		Standard deviation (%)		Strain at maximum strength (%)		Average strain at maximum strength (%)		Standard deviation (%)	
Thinner	Thicker	Normal	Cross	Normal	Cross	Normal	Cross	Normal	Cross	Normal	Cross	Normal	Cross
3.2	6.1	105.2	89.1					3.38	1.65				
3.2	6.1	107.4	97.0	105.9	78.4	1.0	18.4	2.83	2.57	3.1	1.7	0.4	0.6
3.2	6.1	105.7	71.9					2.66	1.46				
3.2	6.1	105.4	55.8					3.36	1.24				

[a]Based on a PBT strength of 59.8 MPa (8.67 ksi).

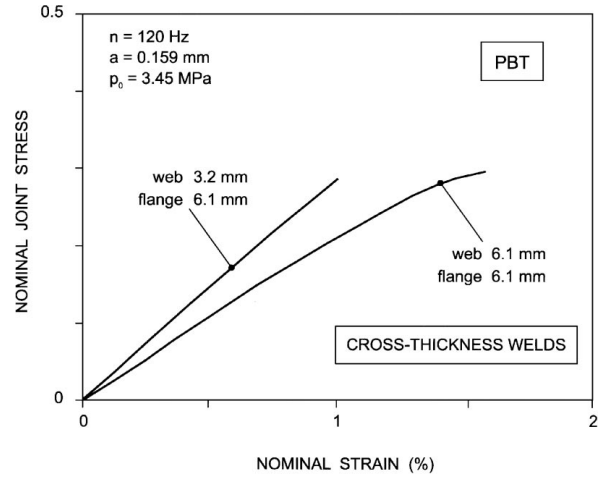

Figure 13 Nominal joint-stress versus nominal strain curves for PBT for (web, flange) thickness combinations of (3.2, 6.1) and (6.1, 6.1) mm.

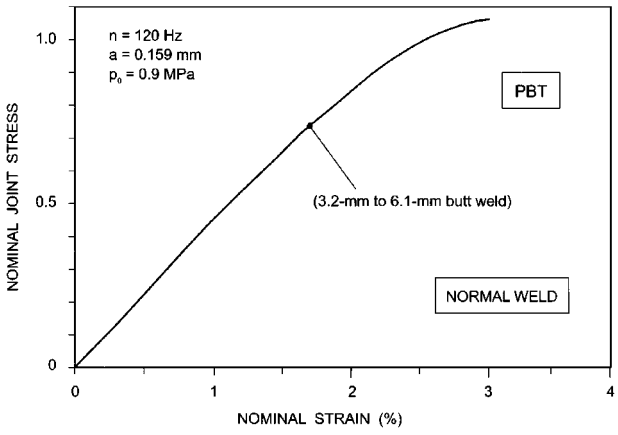

Figure 14 Nominal joint-stress versus nominal strain curves for PBT for unequal thickness butt welds between 3.2- and 6.1-mm specimens.

6.2.2. Unequal thickness butt joints

As in PC, Table VII shows that the strengths of unequal thickness butt welds of PBT are in excess of 90%. This reduction is confirmed by the repeat test data for the (3.2, 6.1) mm web-flange combination, which shows very high repeatable strengths in normal mode welds (Table VIII); the cross-thickness welds exhibit higher variability, however.

The nominal joint stress versus nominal strain plot in Fig. 14—corresponding strength data in row 1 in Table VII—shows that the failure occurs at high strains and stresses in a ductile mode. Thus, as in PC, the drastic reduction in the strengths of PBT T- joints should not be ascribed to the reentrant corners in the joint geometry.

7. Concluding remarks

The test data for the strengths of PC and PBT T-joints clearly show that tests on T-welds do not measure the achievable weld strengths of resins. Not only does this test grossly underestimate the weld strengths of materials, the measured number depends on the absolute and relative thicknesses of the webs and flanges of the T. Thus, a test on a T-joint is a component test, not a test for material weldability. The appropriate geometry for determining the weldability of resins would seem to be that of the butt weld.

The results of tests on T-joints clearly indicate that the stress field at a T-junction in a structure is quite complex. In thermoplastics, in which the strains at failure are very high in comparison to metals, the stress concentration caused by reentrant corners may not be as important a contributor to failure as the subsurface multiaxial stress field—especially in the thin-walled geometries used in thermoplastic parts. These tests point to the need for a more careful examination of the failure mechanism at the junction of a rib and the main structure in an injection molded part. Clearly, an understanding of this failure mechanism would help in designing better welded joints.

Acknowledgements

Support provided by GE Plastics is gratefully acknowledged R. N. Johnson and L. P. Inzinna designed the fixtures for making and testing T-welds, and K. R. Conway carried out all the tests. Their contributions are greatly appreciated.

References

1. V. K. STOKES, *Polym. Eng. Sci.* **28** (1988) 718.
2. *Idem., ibid.* **37** (1997) 715.
3. *Idem., ibid.* **28** (1988) 728.
4. V. K. STOKES and S. Y. HOBBS, *ibid.* **29** (1989) 1667.
5. S. Y. HOBBS and V. K. STOKES, *ibid.* **31** (1991) 502.
6. V. K. STOKES and S. Y. HOBBS, *Polymer* **30** (1993) 1222.
7. V. K. STOKES, *Polym. Eng. Sci.* **31** (1991) 511.
8. *Idem., Polymer* **34** (1993) 4445.
9. *Idem., J. Mater. Sci.* **27** (1992) 5073.
10. *Idem., Polym. Eng. Sci.* **28** (1988) 989.
11. *Idem., ibid.* **28** (1988) 998.

12. *Idem., ibid.* **29** (1989) 1683.
13. *Idem., Polymer* **33** (1992) 1237.
14. P. MICHEL, *Polym. Eng. Sci.* **29** (1989) 1376.
15. A. K. SCHLARB and G. W. EHRENSTEIN, *ibid.* **29** (1989) 1677.
16. V. K. STOKES, *ibid.* **32** (1992) 593.
17. R. P. NIMMER and J. T. WOODS, *ibid.* **32** (1992) 1126.
18. J. T. WOODS and H. G. DELORENZI, *ibid.* **33** (1993) 1431.
19. J. T. WOODS, R. P. NIMMER and K. F. RYAN, *SPE ANTEC Tech. Papers* **41** (1995) 3923.
20. J. T. WOODS and R. P. NIMMER, *SPE ANTEC Tech. Papers* **42** (1996) 3182.

Received 28 June
and accepted 28 November 1999